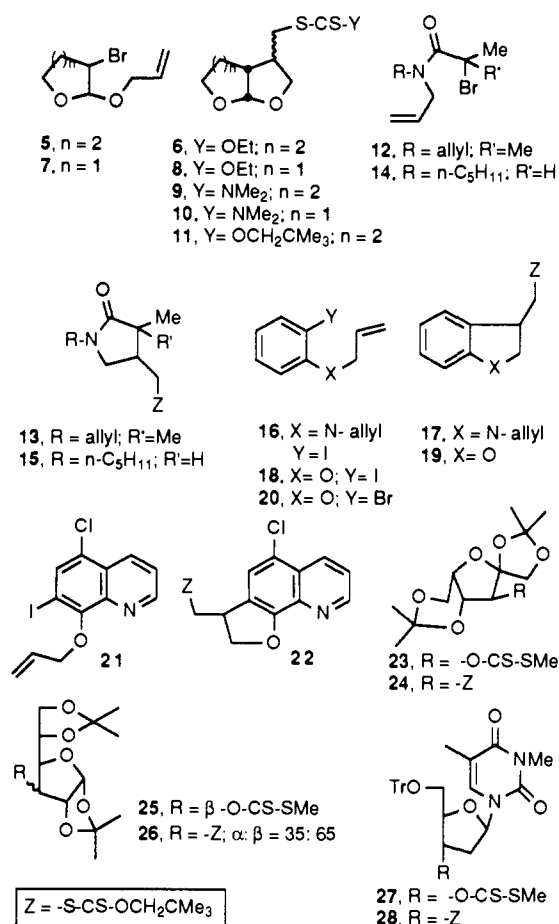


Chart I



potassium *O*-ethyl xanthate. However, it is a low-melting solid which does not keep well, resulting in erratic behavior in some of the experiments. The analogous dithiocarbamate derivative **1b**<sup>7b</sup> was more stable but much less reactive (see Table I, entries 5 and 6). In contrast, the neopentyltin xanthate **1c** turned out to be a stable and effective reagent, giving reproducible results. It is nicely crystalline (mp 94–96 °C) and easily made<sup>7c</sup> and kept. Moreover, we found that addition of a small amount (ca. 10 mol %) of hexabutyliditin or, even better, hexaphenyliditin increased the rate significantly,<sup>7d</sup> presumably by destroying traces of sulfur-containing impurities<sup>8</sup> or side products which can otherwise inhibit the chain reaction.

As shown in the table, a variety of typical radical reactions can be performed using this novel system. In the case of lactam

formation (examples **13** and **15**), no need for high dilution or slow addition of the tin reagent is necessary, in contrast to similar stannane-mediated cyclizations.<sup>9</sup> As would be expected, aromatic bromides were much less reactive than the corresponding iodides (entries 13 and 14). It is also possible to convert an *O*-alkyl xanthate into an *S*-alkyl xanthate as illustrated by examples **24**, **26**, and **28** (entries 16–18) in what appears to be a promising and expedient route to thiosugars and thionucleosides. Some of these derivatives exhibit interesting biological activities and are not always easily accessible by conventional ionic reactions.<sup>10</sup> In the case of **26**, the two epimeric xanthates were shown to interconvert under the reaction conditions, indicating that the xanthate transfer is indeed a reversible process.

We believe that this approach adds a new dimension to tin-based radical methods. Furthermore, since the addition of silyl radicals onto a thiocarbonyl group has also been shown to be reversible,<sup>4c</sup> a similar process should be feasible with the corresponding silicon xanthates.

**Acknowledgment.** We thank Dr. B. Quiclet-Sire for a gift of tritylthymidine and Dr. J.-L. Fourrey for helpful discussions.

**Registry No.** **1a**, 22703-09-9; **1b**, 1803-12-9; **1c**, 143037-51-8; **5**, 73746-50-6; **6** (isomer 1), 143037-52-9; **6** (isomer 2), 143119-80-6; **7**, 143037-46-1; **8** (isomer 1), 143037-53-0; **8** (isomer 2), 143119-81-7; **9** (isomer 1), 143037-54-1; **9** (isomer 2), 143119-82-8; **10** (isomer 1), 143037-55-2; **10** (isomer 2), 143119-83-9; **11** (isomer 1), 143037-56-3; **11** (isomer 2), 143119-84-0; **12**, 39089-47-9; **13**, 143037-57-4; **14**, 143037-47-2; *cis*-**15**, 143037-58-5; *trans*-**15**, 143037-59-6; **16**, 73396-92-6; **17**, 143037-60-9; **18**, 24892-63-5; **19**, 143037-61-0; **20**, 60333-75-7; **21**, 123552-78-3; **22**, 143037-62-1; **23**, 143037-48-3; **24**, 143037-63-2; **25**, 143037-49-4;  $\alpha$ -**26**, 143037-64-3;  $\beta$ -**26**, 143037-65-4; **27**, 143037-50-7; **28**, 143037-66-5.

(9) Stork, G.; Mah, R. *Heterocycles* **1989**, *28*, 723. (b) Clough, J. M.; Pattenden, G.; Wight, P. G. *Tetrahedron Lett.* **1989**, *30*, 7469. (c) Jolly, R. S.; Livinghouse, T. J. *Am. Chem. Soc.* **1988**, *110*, 7537. (d) Sato, T.; Wada, Y.; Nishimoto, M.; Ishibashi, H.; Masazumi, I. *J. Chem. Soc., Perkin Trans. I* **1989**, 879.

(10) (a) Buchanan, J. G.; Wightman, R. H. In *Topics in Antibiotic Chemistry*; Sammes, P., Ed.; Ellis Harwood: Chichester, 1982; Vol. 6, p 229. For some recent references on the preparation of thiosugars and thionucleosides, see: (b) Cicero, D.; Varela, O.; de Lederkremer, R. M. *Tetrahedron* **1990**, *46*, 1131. (c) Marriot, J. H.; Mottahedeh, M.; Reese, C. B. *Carbohydr. Res.* **1991**, *216*, 257; *Tetrahedron Lett.* **1990**, *31*, 7485. (d) Li, X.; Andrews, D. M.; Cosstick, R. *Tetrahedron* **1992**, *48*, 2729.

### Synthesis of an Equilateral Triangular Molybdenum Cluster Complex [Mo<sub>3</sub>( $\mu$ -S)<sub>2</sub>( $\mu$ -S)<sub>3</sub>(PMe<sub>3</sub>)<sub>6</sub>] with Eight Cluster Valence Electrons

Kiyoshi Tsuge, Setsuko Yajima, Hideo Imoto, and Taro Saito\*

Department of Chemistry, Faculty of Science  
The University of Tokyo, Hongo, Tokyo, 113, Japan

Received March 6, 1992

Several structural types of trinuclear molybdenum cluster complexes have been reported, and the relationship between their geometrical and electronic structures has been an important subject of intensive studies.<sup>1</sup> In the present communication, we report a new cluster complex [Mo<sub>3</sub>( $\mu$ -S)<sub>2</sub>( $\mu$ -S)<sub>3</sub>(PMe<sub>3</sub>)<sub>6</sub>] (**I**) containing a "Mo<sub>3</sub>S<sub>5</sub>" unit with two capping and three edge-bridging sulfur ligands. The unit is the first member of the series Mo<sub>3</sub>nS<sub>3n+2</sub>

(7) (a) Schmidt, M.; Schumann, H.; Gliniecki, F.; Jaggard, J. F. *J. Organomet. Chem.* **1969**, *17*, 277. (b) Domazetis, G.; Magee, R. G.; James, B. D. *J. Organomet. Chem.* **1977**, *141*, 57. (c) Preparation of **1c**: Chlorotriphenyltin (21.2 g, 55 mmol) was added at room temperature to a stirred solution of sodium *O*-neopentyl xanthate (10 g, 54 mmol) (Johansson, A. *Ark. Kemi Mineral. Geol.* **1946**, *B22*, 7; *Chem. Abstr.* **1947**, *41*, 1209e) in 100 mL of dry acetone. The reaction mixture was allowed to stir at room temperature for 3 h and then filtered, and the filtrate was evaporated to dryness. The residue was recrystallized from diethyl ether-pentane to give **1a** as almost white crystals: yield 19.8 g, 72%; mp 94–96 °C; IR (CH<sub>2</sub>Cl<sub>2</sub>, cm<sup>-1</sup>) 3046, 2963, 1479, 1429, 1223, 1071; <sup>1</sup>H NMR (200 MHz, CDCl<sub>3</sub>) 7.7 and 7.4 (m, 15 H), 4.01 (s, 2 H), 0.86 (s, 9 H); <sup>13</sup>C NMR (50 MHz, CDCl<sub>3</sub>, ppm) 216.2, 138.6, 136.8, 129.8, 128.9, 85.63, 31.71, 26.45; MS *m/z* (M<sup>+</sup>) calcd 514.0447, obsd 514.0439. (d) Typical experimental procedure: Argon was bubbled through a suspension of the substrate (1 mmol), **1c** (2 mmol), and Ph<sub>3</sub>Sn<sub>2</sub> (0.15 mmol) in 5 mL of dry cyclohexane for 15 min. The mixture was then irradiated with visible light (500-W tungsten lamp) for the time specified in the table (the heat from the lamp caused the solvent to reflux). The reaction mixture was then concentrated in vacuo and the residue purified by silica gel chromatography.

(8) Ditin derivatives are known to react with disulfides and other sulfur compounds, see: Neumann, W. P. *The Organic Chemistry of Tin*; J. Wiley: New York, 1970. The role of the ditin in our case is probably analogous to that played in reactions involving iodine atom transfer: Curran, D. P.; Chen, M.-H.; Kim, D. *J. Am. Chem. Soc.* **1989**, *111*, 6265.

(1) (a) Müller, A.; Jostes, R.; Cotton F. A. *Angew. Chem., Int. Ed. Engl.* **1980**, *19*, 875. (b) Burnsten, B. E.; Cotton, F. A.; Hall, M. B.; Najjar, R. C. *Inorg. Chem.* **1982**, *21*, 302. (c) Cotton, F. A.; Feng, X. *Inorg. Chem.* **1991**, *30*, 3666. (d) Cotton, F. A.; Shang, M.; Sun, Z. S. *J. Am. Chem. Soc.* **1991**, *113*, 3007. (e) Cotton, F. A.; Shang, M.; Sun, Z. S. *J. Am. Chem. Soc.* **1991**, *113*, 6917. (f) Cotton, F. A.; Kibala, P. A.; Miertschin, C. S. *Inorg. Chem.* **1991**, *30*, 548.

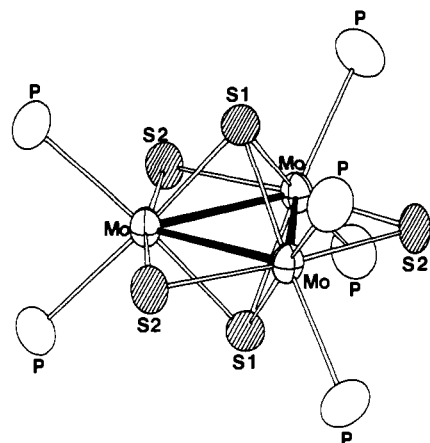


Figure 1. ORTEP drawing of  $[\text{Mo}_3\text{S}_3(\text{PMe}_3)_6]$  with 50% probability ellipsoids. Carbon and hydrogen atoms have been omitted.

constructed from a stack of  $\text{Mo}_3$  triangles in a staggered fashion. The higher members ( $n \geq 2$ ) of the series are the building blocks of the superconducting Chevrel phases,<sup>2</sup> and a molecular complex containing the octahedral  $\text{Mo}_6\text{S}_8$  unit ( $n = 2$ ) has been reported by us.<sup>3</sup>

The cluster complex I was prepared by the treatment of  $(\text{NH}_4)_2\text{Mo}_3\text{S}_3$ <sup>4</sup> with excess trimethylphosphine in tetrahydrofuran at room temperature. A black crystalline product was isolated in 26% yield. A visible spectrum in  $\text{CH}_2\text{Cl}_2$  shows absorptions at  $\lambda_{\text{max}}/\text{nm}$  ( $\epsilon/(10^3 \text{ M}^{-1} \text{ cm}^{-1})$ ) 368 (3.4), 447 (4.0), 565 (2.0), and 780 (0.3). A <sup>31</sup>P NMR spectrum shows a sharp singlet at  $\delta$  30.4 (85%  $\text{H}_3\text{PO}_4$  as an external reference). A <sup>1</sup>H NMR spectrum in  $\text{CDCl}_3$  gives a broad singlet at  $\delta$  1.4. Cyclic voltammetry in the  $\text{CH}_2\text{Cl}_2$  solution has indicated a quasi-reversible reduction wave at  $E_{1/2} = -1.16 \text{ V}$  and a quasi-reversible oxidation wave at  $E_{1/2} + 0.06 \text{ V}$  (vs  $\text{Ag}/\text{AgNO}_3$  (0.01 M in  $\text{CH}_3\text{CN}$ )).<sup>5</sup>

The X-ray crystal structure determination<sup>6</sup> of I has revealed the structure illustrated in Figure 1. The cluster has an equilateral triangle of three molybdenum atoms capped by two sulfur atoms and bridged by three sulfur atoms. Two trimethylphosphines are coordinated to each molybdenum atom. There is a crystallographically imposed 3-fold axis through the cluster, and the overall molecular structure has a  $D_3$  symmetry slightly distorted from the  $D_{3h}$  symmetry, with distances  $\text{Mo}-\text{Mo}$  2.714 (1) Å,  $\text{Mo}-\mu_3\text{-S}$  2.421 (1) Å, and  $\text{Mo}-\mu\text{-S}$  2.393 (1) Å.

The electronic structures of several types of triangular molybdenum cluster complexes have been calculated and discussed. If we assume 3-fold symmetry, triangular clusters have two low-lying orbitals consisting primarily of molybdenum 4d orbitals, which are an  $a_1$  (or  $a_1'$ ) and an  $e$  (or  $e'$ ) orbital.<sup>1</sup> If a cluster has six metal electrons, these orbitals are occupied and the cluster is electron-precise. However, it depends on the structure whether the next lower metallic orbital is degenerate or not.<sup>1</sup> Therefore, the Jahn-Teller distortion can operate in some of the eight-electron clusters.

The disposition of the atoms in I is similar to that in  $[\text{Mo}_3(\mu_3\text{-S})_2(\mu\text{-Cl})_3\text{Cl}_6]^{3-}$  (II)<sup>7</sup> and in  $[\text{Cr}_3(\mu_3\text{-S})_2(\mu\text{-S})_3-$

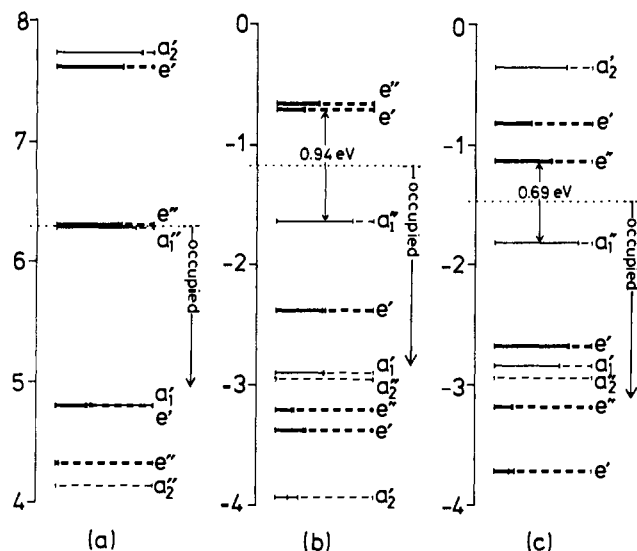


Figure 2. Energy levels of (a)  $[\text{Mo}_3(\mu_3\text{-S})_2(\mu\text{-Cl})_3\text{Cl}_6]^{3-}$ , (b)  $[\text{Mo}_3(\mu_3\text{-S})_2(\mu\text{-S})_3(\text{PH}_3)_6]$ , and (c)  $[\text{Cr}_3(\mu_3\text{-S})_2(\mu\text{-S})_3(\text{PH}_3)_6]$  calculated by the DVX $\alpha$  method. Degenerate levels are drawn with thicker lines than those for nondegenerate levels. The metal constitution for each orbital is shown with a continuous line while the total contribution from nonmetal orbitals is indicated with a broken line.

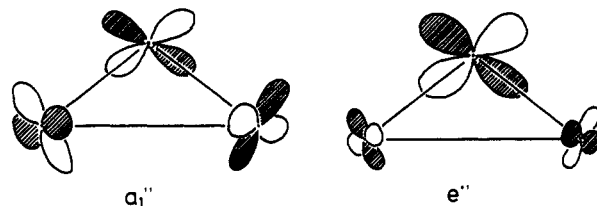


Figure 3. Schematic drawings of the molecular orbitals of the  $a_1''$  (HOMO) and the  $e''$  symmetry for  $[\text{Mo}_3\text{S}_3(\text{PMe}_3)_6]$ .

$(\text{Me}_2\text{PC}_2\text{H}_4\text{PMe}_2)_3$  (III).<sup>8</sup> The edge-bridging and terminal ligands in II are chlorines instead of sulfur and trialkylphosphine as in I and III. All of these clusters have the same metal oxidation state (+3.33) and eight cluster electrons. However, in contrast to the equilateral triangular core of I, the triangular metal cores in II and III are distorted to isosceles triangles with a shorter (II) or a longer (III) base. According to the electronic structure calculation by Jiang and others, the cluster II should have a degenerate HOMO ( $e''$ ) occupied by two electrons if II had the perfect  $D_{3h}$  symmetry.<sup>7</sup> The distortion has been accounted for in terms of the Jahn-Teller effect. On the other hand, Arif and others have obtained the results of the calculation in which the chromium cluster III in the  $D_{3h}$  symmetry has a nondegenerate HOMO ( $a_1''$ ), and they argued that the distortion observed in spite of the nondegeneracy of the HOMO may be due to the second-order Jahn-Teller effect which mixes the HOMO ( $a_1''$ ) and the LUMO ( $e''$ ).<sup>8</sup>

To elucidate the reason why the  $\text{Mo}_3$  triangle in I is not distorted, we have calculated the molecular orbitals of model complexes  $[\text{Mo}_3(\mu_3\text{-S})_2(\mu\text{-S})_3(\text{PH}_3)_6]$  (I'),  $[\text{Mo}_3(\mu_3\text{-S})_2(\mu\text{-Cl})_3\text{Cl}_6]^{3-}$  (II'), and  $[\text{Cr}_3(\mu_3\text{-S})_2(\mu\text{-S})_3(\text{PH}_3)_6]$  (III') by the DVX $\alpha$  method.<sup>9</sup>  $D_{3h}$  symmetry has been assumed for all the complexes. In all of the clusters I', II', and III', either the  $e''$  or the  $a_1''$  orbital is the HOMO (Figure 2). The  $a_1''$  and  $e''$  levels of II' have very similar

(2) Chevrel, R.; Sergent, M. In *Superconductivity in Ternary Compounds I*; Fisher, O., Maple, M. B., Eds.; Springer-Verlag: Berlin, 1982; p 25.

(3) Saito, T.; Yamamoto, N.; Nagase, T.; Tsuboi, T.; Kobayashi, K.; Yamagata, T.; Imoto, H.; Unoura, K. *Inorg. Chem.* 1990, 29, 764.

(4) (a) Müller, A.; Sarkar, S.; Bhattacharyya, R. G.; Pohl, S.; Dartmann, M. *Angew. Chem., Int. Ed. Engl.* 1978, 17, 535. (b) Müller, A.; Krickemeyer, E. *Inorg. Synth.* 1990, 27, 47-48.

(5) Tetrabutylammonium perchlorate (0.1 M) was used as the supporting electrolyte. The measurement was made at 17 °C in a  $\text{CH}_2\text{Cl}_2$  solution by using a platinum electrode with a scan rate of 100 mV/s. Ferrocene (2 mM in  $\text{CH}_2\text{Cl}_2$ ) gave an oxidation wave at  $E_{1/2} = +0.46 \text{ V}$  under the same conditions.

(6) Crystal data: space group  $R\bar{3}c$  with  $a = 11.112$  (1) Å,  $c = 53.507$  (10) Å,  $V = 5722$  (1) Å<sup>3</sup>, and  $Z = 6$ . The structure was solved by direct methods and Fourier syntheses (SHELXS76 and SHELXS86) and refined with an isotropic extinction correction (ANYBLK).  $R = 0.043$  and  $R_w = 0.026$  for 1534 observed reflections ( $F > 3.0\sigma(F)$ ) with  $2\theta < 60^\circ$  ( $\text{Mo K}\alpha$  radiation).

(7) (a) Jiang, Y.; Tang, A.; Hoffmann, R.; Huang, J.; Lu, J. *Organometallics* 1985, 4, 27. (b) Huang, J.; Shang, M.; Lui, S.; Lu, J. *Sci. Sin., Ser. B (Engl. Ed.)* 1982, 25, 1270. (c) Huang, J.; Shang, M.; Huang, J.; Lu, J. *Proceedings of the 2nd China-Japan-U.S.A. Symposium on Organometallic and Inorganic Chemistry*, 1982; p 38.

(8) Arif, M. A.; Hefner, J. G.; Jones, R. A.; Albright, T. A.; Kang, S.-K. *J. Am. Chem. Soc.* 1986, 108, 1701.

(9) The program used was written by H. Adachi. (a) Adachi, H.; Tsukada, M.; Satoko, C. *J. Phys. Soc. Jpn.* 1978, 45, 875. (b) Satoko, C.; Tsukada, M.; Adachi, H. *J. Phys. Soc. Jpn.* 1978, 45, 1333. (c) Adachi, H.; Shiokawa, S.; Tsukada, M.; Satoko, C.; Sugano, S. *J. Phys. Soc. Jpn.* 1979, 47, 1528.

energies, and its structure will be distorted due to the Jahn-Teller effect. On the other hand, the  $a_1''$  level is lower than  $e''$  in I and III, yielding a nondegenerate HOMO. These results are consistent with previous extended Hückel calculations as mentioned above.<sup>7a,8</sup>

The order of the  $a_1''$  and  $e''$  levels seems to be determined mainly by the antibonding  $\pi$ -interaction between the molybdenum 4d orbitals and the filled 3p orbitals of the bridging ligand atoms. These orbitals are derived from the same type of molybdenum 4d orbitals as shown in Figure 3. The interaction destabilizes only the  $e''$  orbital because the  $a_1''$  does not interact with the p orbitals due to the mismatch in symmetry. Since sulfur is less electronegative than chlorine, the energies of its 3p orbitals are closer to those of the molybdenum 4d orbitals. Therefore, the sulfur ligands in I' and III' are expected to have stronger  $\pi$ -interactions with metal d orbitals, and to destabilize the  $e''$  orbital more than the chlorine ligands in II'.

As shown in Figure 2, I' and III' have very similar energy level diagrams in the HOMO-LUMO region except that the three highest occupied orbitals have more metallic character in III' than in I'. Our preliminary calculation has also shown that the electronic levels of I' change similarly to those of III' when the structures are distorted in the  $C_{2v}$  symmetry in such a way as observed in III. Especially, the HOMO  $a_1''$  orbital is influenced very little by the distortion in both compounds. Therefore, the electronic structures of I and III should be very similar though only III exhibits distortion of the metal triangle in the X-ray structure analysis. The interplay of electronic and steric influences that distorts III may be very delicate and/or complex. However, the lack of distortion in I can be explained straightforwardly by the nondegeneracy of the HOMO.

**Acknowledgment.** Support from the Ministry of Education, Science and Culture of Japan (Grants-in-Aid for Scientific Research 02453037, 03233207) is gratefully acknowledged.

**Supplementary Material Available:** Tables SI-SIV containing listings of crystallographic data, atomic parameters, anisotropic thermal parameters, and bond distances and angles for compound I (5 pages); listing of observed and calculated structure factors for compound I (10 pages). Ordering information is given on any current masthead page.

## Use of Nuclear Potential To Investigate the "Atomic Size" Dependency of Populations Defined within the Theory of Atoms in Molecules

Keith E. Laidig

University Chemical Laboratory  
Lensfield Road, Cambridge, CB2 1EW, U.K.  
Received December 9, 1991

A recent publication<sup>1</sup> has criticized results obtained using the theory of atoms in molecules<sup>2</sup> by claiming that the "atomic size" dependency of the form of the charge distribution leads to erroneous and unaccountable errors in the predictions of the theory. The interpretation of the behavior of simple model systems is used to claim that the location of the zero-flux surface depends upon atomic orbital size. These models are the foundations of the critical arguments that follow regarding the exaggeration of the atomic populations predicted by the theory of atoms in molecules and consequently their unreliability as a basis for the investigation of physical phenomena.

The second model presents a "1:1 LCAO-MO" model which "localizes a known, and preferably equal, electron population on

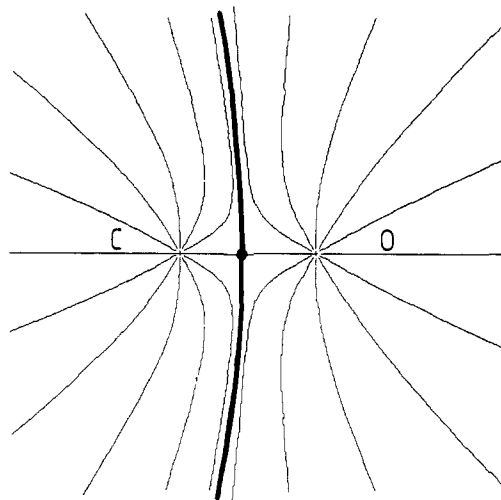


**Figure 1.** Gradient vector field of the nuclear potential of the system as defined in eq 1. The surface of balanced forces between the two nuclei has been darkened for emphasis, the intersection of this surface with the internuclear axis is represented by a black dot, and the position of each nucleus is represented by a cross.

each atom".<sup>1</sup> A system with carbon and oxygen separated by 2.70 bohr is presented with each nucleus having a Slater sp hybrid atomic orbital. One electron is put into this system, and the resulting distribution produces a critical point (the point at which the charge density reaches a minimum along the interatomic axis) closer to the carbon nucleus than to the oxygen along the interatomic axis. An integration is performed within the regions bounded by the zero-flux surface in the gradient vector field, and the atomic populations are determined, with the carbon atom having 0.30 and the oxygen 0.70 of the electronic charge. The author claims that the failure to distribute the population equally between the two atoms demonstrates the "atomic size" dependency and hence the weakness of the theory of atoms in molecules.

The implicit assumption used above is that the amount of charge should be evenly divided between the two atoms of this system. We propose a simple consideration of the nuclear potential<sup>3</sup> between these two atoms to demonstrate that this cannot be so. The nuclear potential generates the nuclear-electron attraction, the dominant force within a molecular system, and is responsible for the form of the molecular distribution.<sup>3</sup> The nuclear potential, for a given nuclear configuration,  $X$ , with nuclear charges,  $Z_\alpha$ , is defined as

$$V(r;X) = \sum_{\alpha} Z_{\alpha} (|r - X_{\alpha}|)^{-1} \quad (1)$$

Given the model system described above, one finds the nuclear potential, as displayed by its gradient vector field, has the form found in Figure 1. The lines shown in the figure are those of force (the gradient of the potential), i.e., lines along which a negative test charge moves under the influence of the nuclear potential. The system is divided into two regions of space in which the lines of force lead to one nucleus or the other, i.e., regions of space in which a test charge is dominated by the potential of that nucleus. Figure 1 shows that the region of space in which the test charge is dominated by oxygen is larger than that for carbon. The form of the distribution of one electron under the influence of this potential will not have an equal amount of charge on each atom, and integration of the atomic populations of such a distribution should yield a larger population for oxygen.

In between these regions there is a surface in three dimensions on which the force on a test charge is equally balanced between the two nuclei. This surface of balanced force is not midway along

(1) Perrin, C. L. *J. Am. Chem. Soc.* **1991**, *113*, 2865.

(2) Wiberg, K. B.; Laidig, K. E. *J. Am. Chem. Soc.* **1987**, *109*, 5935. Wiberg, K. B.; Laidig, K. E. *J. Am. Chem. Soc.* **1988**, *110*, 1872. Wiberg, K. B.; Schriber, S. L. *J. Org. Chem.* **1988**, *53*, 783. Wiberg, K. B.; Breneman, C. M.; Le Page, T. J. *J. Org. Chem.* **1990**, *112*, 61. Wiberg, K. B. *J. Am. Chem. Soc.* **1990**, *112*, 4177. Siggel, M. R. F.; Streitwieser, A., Jr.; Thomas, T. D. *J. Am. Chem. Soc.* **1988**, *110*, 8022.

(3) Tal, Y.; Bader, R. F. W.; Erkkü, J. *Phys. Rev.* **1980**, *A21*, 1. Parr, R. G.; Berk, A. In *Chemical Applications of Atomic and Molecular Electrostatic Potentials*; Politzer, P., Truhlar, D. G., Eds.; Plenum Press: New York, 1981; p 51. Bader, R. F. W. *Atoms in Molecules: A Quantum Theory*; Oxford University Press: Oxford, 1990.